

# Dark matter halo concentrations with a bayesian approach

Christian Poveda<sup>1</sup> & Jaime E. Forero-Romero<sup>1</sup>

<sup>1</sup>*Departamento de Física, Universidad de los Andes, Cra. 1 No. 18A-10, Edificio Ip, Bogotá, Colombia*

13 September 2014

## ABSTRACT

asd

**Key words:** methods: numerical, galaxies: haloes, cosmology: theory, dark matter

## 1 INTRODUCTION

(Navarro et al. 1997)

## 2 BASIC PROPERTIES OF THE NFW DENSITY PROFILE

The Navarro-Frenk-White density profile can be written as

$$\rho(r) = \frac{\rho_c \delta_c}{r/r_s (1 + r/r_s)^2}, \quad (1)$$

where  $\rho_c \equiv 3H^2/8\pi G$  is the Universe critical density,  $\delta_c$  is the halo dimensionless characteristic density and  $r_s$  is known as the scale radius, the radius that marks the transition between the two power law behaviour in the  $\rho \propto r^{-1}$  for  $r < r_s$  and  $\rho \propto r^{-3}$  for  $r > r_s$ .

We define the virial radius of a halo,  $r_v$ , as the boundary of the spherical volume that encloses an average density of  $\Delta_h$  times the average density of the Universe. The corresponding mass  $M_v$ , the virial mass, can be written as  $M_v = \frac{4\pi}{3} \bar{\rho} \Delta_h r_v^3$ .

### 2.1 Integrated Mass

From these definitions we can compute the total mass enclosed inside a radius  $r$ :

$$M(< r) = 4\pi \rho_c \delta_c r_s^3 \left[ \ln \left( \frac{r_s + r}{r} \right) - \frac{r}{r_s + r} \right]. \quad (2)$$

We can now express the same quantity in terms of dimensionless the variables  $x \equiv r/r_v$  and  $m \equiv M(< r)/M_v$ ,

$$m(< x) = \frac{1}{A} \left[ \ln(1 + xc) - \left( \frac{xc}{xc + 1} \right) \right], \quad (3)$$

where

$$A = \left[ \ln(1 + c) - \left( \frac{c}{c + 1} \right) \right], \quad (4)$$

and the parameter  $c$  is known as the concentration  $c \equiv r_v/r_s$ .

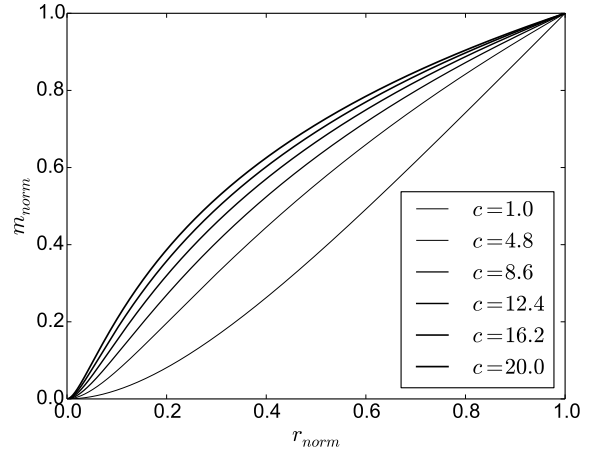


**Figure 1.** Dimensionless mass profiles as a function of the dimensionless radius for different concentration values.

The most interesting feature of Eq. (3) is that the concentration is the only free parameter to describe the shape of the halo density profile. In Figure 1 we show  $m(< x)$  as a function of  $x$  for different values of the concentration in the range  $1 \leq c \leq 20$ .

### 2.2 Circular velocity

It is also customary to express the mass of the halo in terms of the circular velocity  $V_c = \sqrt{GM(< r)/r}$ . From this we can define a new dimensionless circular velocity  $v(< x) \equiv V_c(< r)/V_c(< r_v)$ , using the result in Equation 3 to have:

$$v(< x) = \sqrt{\frac{1}{A} \left[ \frac{\ln(1 + xc)}{x} - \frac{c}{xc + 1} \right]}, \quad (5)$$

### 3 A BAYESIAN APPROACH TO HALO FITTING

We proceed to find the value of the concentration parameter that best describes the simulation data, following the model in Eq. (3). We use the integrated mass profile because it allows us to use the data directly with the simulation without binning the particle positions and estimating a density.

We construct the integrated mass profile by ranking the particles by their increasing distance to the center of the halo. Once they are ranked, the total mass at a radius  $r_i$ , increases by  $m_p$ , where  $r_i$  is the position of the  $i$ -th particle and  $m_p$  is the mass of the computational particle. We define the center of the halo to be at the position of the particle with the lowest gravitational potential. In the process of building the mass profile we discard the particle at the center.

We stop the construction of the integrated mass profile once we arrive at an average density of  $\Delta_h \bar{\rho}$ . This radius marks the virial radius and the virial mass. We divide the total mass enclosed mass  $M_i$  and the radii  $r_i$  by these values to obtain the dimensionless variables  $x_i$  and  $m_i$ .

Using these positions and masses we define the following  $\chi^2$  function

$$\chi^2(c) = \sum_i [\log m_i - \log m(< x_i; c)]^2, \quad (6)$$

where  $m(< x_i; c)$  corresponds to the values in Eq.(3) at  $x = x_i$  and a given value of the concentration parameter  $c$ .

Finally we use a Metropolis-Hastings algorithm to sample the likelihood function distribution defined by  $\mathcal{L}(c) = \exp(-\chi^2(c)/2)$  to find the optimum value of  $c$  and its associated uncertainty  $\sigma_c$ .

## 4 NUMERICAL EXPERIMENTS

### 4.1 Mock Halos

We generate 100 mock halos with concentration values randomly placed in the range  $1 < c < 20$ . Each one of the halos is generated with four different total particle numbers: 20, 200, 2000 and 20000.

The method we use to generate the halos is based on the integrated mass profile. Given the number of particles  $n$  and the concentration  $c$  we define the mass element as  $\delta m = 1/n$  (this corresponds to the mass of each particle such that the total mass is one). Then for each number  $k$  from 1 to  $n$  we find the value of  $r$  such that the difference

$$m(< r; c) - k \cdot \delta m \quad (7)$$

is zero using Ridders' method. This value of  $r$  is the radius of the  $k$ th particle of the generated halo, then polar and azimuthal angles  $\theta$  and  $\phi$  are randomly generated. Finally these three coordinates are transformed into cartesian coordinates  $(r, \theta, \phi) \rightarrow (x, y, z)$ . This process is repeated  $n$  times in order to generate the  $x, y, z$  coordinates for each particle.

### 4.2 Simulation Data

We use data from the MultiDark cosmological volume. This simulation follows the non-linear evolution of a dark matter

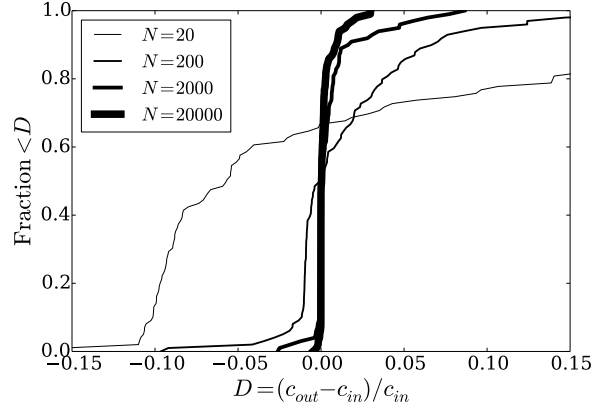


**Figure 2.** Cumulative distribution of the fractional difference between the input concentration in the mock halo generator,  $c_{in}$  and the measurement by our MCMC code,  $c_{out}$ . Each curve corresponds to halos generated with a different number of particles,  $N$ .

density field sampled with 2048<sup>3</sup> particles over a cubic box of 1000  $h^{-1}$ Mpc on a side. The data is publicly available, more details about the structure of the database and the simulations can be found in (Riebe et al. 2013).

We select a sample of halos in a cubic sub-volume of 100  $h^{-1}$ Mpc on a side centered on the most massive halo in the simulation at  $z = 0$ <sup>1</sup>. We select first all the halos at  $z = 0$  detected with a Friends-of-Friends (FoF) algorithm with masses in the interval  $10^{11} \leq M_{\text{FoF}}/h^{-1}M_{\odot} \leq 10^{15}$ . The FoF algorithm ran with a linking length of 0.17 times the average interparticle distance. This choice translates into an overdensity  $\Delta_h \sim 400 - 700$  that is dependent on the halo concentration (More et al. 2011).

For each selected halo with the previous procedure we select from the database all the particles that belong to it. From the particles we follow the procedure spelled out in Section 3 with  $\Delta_h = 740$  (corresponding to 200 times the critical density) to find the halo concentration. Finally, we store the values obtained for the virial radius, virial mass and concentration.

## 5 RESULTS

### 5.1 Mock Halos

In Figure 2 we show the integrated distribution percentual difference between the concentration measured with our fitting method  $c_{out}$  in comparison with the concentration used to generate the mock halos,  $c_{in}$ ,  $D = (c_{in} - c_{out})/c_{in}$ . Then we can see that as the number of particles increases, the curve becomes more pronounced at 0. Showing that for most of the halos  $c_{in}$  is very similar to  $c_{out}$ .

<sup>1</sup> This corresponds to the **miniMDR1** database in the MultiDark webpage

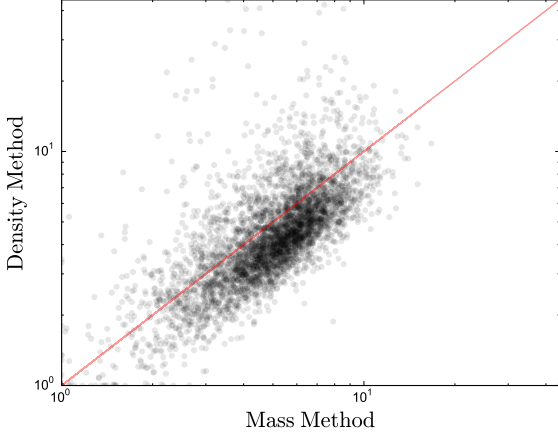


**Figure 3.** Concentration obtained from the density method against the one obtained in the mass method

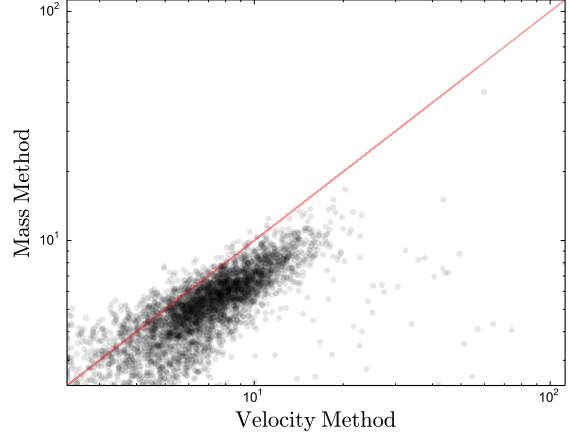


**Figure 5.** Concentration obtained from the mass method against the one obtained in the velocity method

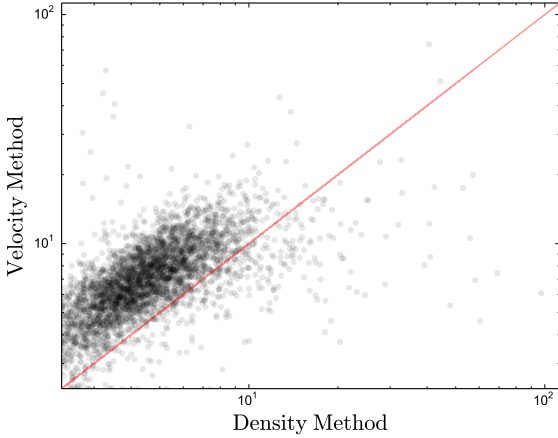


**Figure 4.** Concentration obtained from the velocity method against the one obtained in the density method

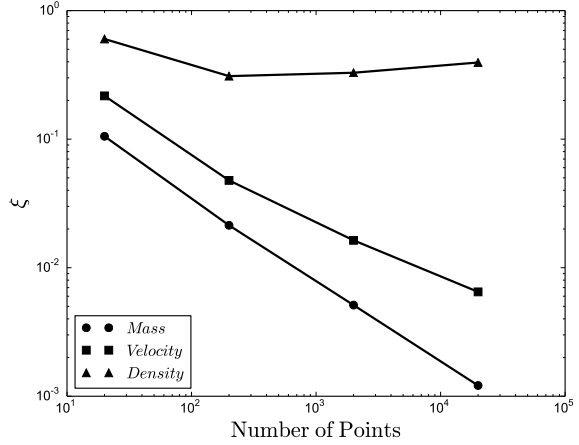


**Figure 6.** Relative error Against number of Particles

## 5.2 Simulation Data

## 6 DISCUSSION

### 6.1 Comparison against other methods

We compared this method against two methods: The first one consists in using shells for estimating the density in function of the radius and using the same MCMC method for fitting and the second one consists in using the circular velocity  $V(r) = \sqrt{GM(<r)/r}$  and the relation for the NFW profile

$$\frac{V_{max}}{V(r_v)} = \sqrt{\frac{0.216c}{M(r_v; c)}} \quad (8)$$

Where  $V_{max}$  is the maximum velocity, to find the value of the concentration.

We tested the three methods using the same data from the Mock Halos test. In order to see the accuracy of each method depending on the number of particles we define

$$\xi(n) = \frac{1}{|\mathcal{H}_n|} \sum_{\mathcal{H}_n} \left| \frac{c_{org} - c_{obt}}{c_{org}} \right| \quad (9)$$

Where  $\mathcal{H}_n$  corresponds to the set of haloes with  $n$  particles,  $c_{org}$  and  $c_{obt}$  are the original and obtained concentrations respectively for each halo in  $\mathcal{H}_n$  and  $|\mathcal{H}_n|$  the number of haloes in  $\mathcal{H}_n$ . Then we calculate  $\xi$  for each number of particles (20, 200, 2000 and 20000).

In Figure 6 we plotted  $\xi$  for the three methods. We consider that  $\xi$  is a good estimate because it is standardized, giving equal weight to all errors regardless of the magnitude of the concentrations or the number of halos. On the other hand we have that  $\xi$  decreases quite fast with the number of particles for our method and is more precise in any case than the other methods.

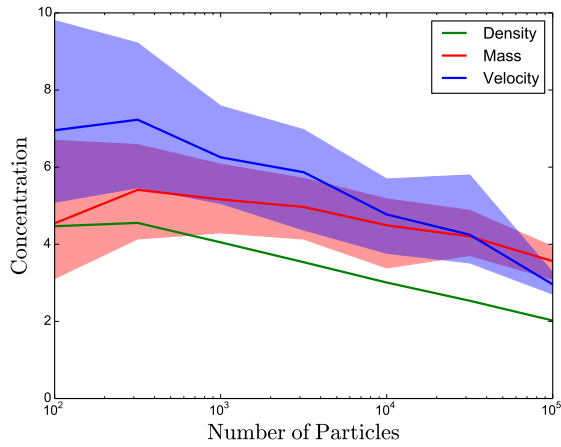


**Figure 7.** Concentration against number of particles

## 6.2 Concentration as a function of halo mass

Additionally we compared those three methods plotting the concentration as a function of the number of particles of each halo

The bold lines in Figure 7 corresponds to the median and the thinner lines corresponds to the quartiles.

## 6.3 Implication for comparisons against observations

FIXME: Ask to Jaime

## 7 CONCLUSIONS

FIXME: Ask to Jaime

## REFERENCES

- More S., Kravtsov A. V., Dalal N., Gottlöber S., 2011, *ApJS*, 195, 4
- Navarro J. F., Frenk C. S., White S. D. M., 1997, *ApJ*, 490, 493
- Riebe K., Partl A. M., Enke H., Forero-Romero J., Gottlöber S., Klypin A., Lemson G., Prada F., Primack J. R., Steinmetz M., Turchaninov V., 2013, *Astronomische Nachrichten*, 334, 691